IV International Conference on Particle-based Methods – Fundamentals and Applications
PARTICLES 2015
E. Oñate, M. Bischoff, D.R.J. Owen, P. Wriggers & T. Zohdi (Eds)

VIRTUAL CONCRETE SPECIMENS: DISCRETE ELEMENT SIMULATIONS OF THE QUASISTATIC AND DYNAMIC MATERIAL BEHAVIOR AND FAILURE MECHANISMS OF CONCRETE AND MORTAR

DIRK S. REISCHL[1] AND MANFRED CURBACH[2]

[1] Faculty of Civil Engineering, Institute of Concrete Structures
Technische Universität Dresden
George-Bähr-Str. 1, 01069 Dresden, Germany
Dirk.Reischl@tu-dresden.de

[2] Faculty of Civil Engineering, Institute of Concrete Structures
Technische Universität Dresden
George-Bähr-Str. 1, 01069 Dresden, Germany
Manfred.Curbach@tu-dresden.de

Key words: Granular Materials, DEM, Contact Problems

Abstract. A quite minimalistic approach is described which allows to generate differently shaped ensembles of densely packed spherical particles. The distributions of the particle diameters approximate realistic sieving distributions of concrete aggregates. An ad hoc approach is used in order to add cohesive interaction forces to the model which allows first plausibility tests.

1 INTRODUCTION

Real experiments to investigate the damage behavior of concrete provide insight into the damage behavior of the specimens used and, after having carried out a sufficient number of experiments, into the damage behavior of the material itself. However, such experiments always imply destruction and non-reusability. The generation of representative, standardized specimens is a non-trivial task and the application of similar loading scenarios in the testing machine requires considerable skill and care.

Virtual specimens are destructible and indestructible at the same time. Each individual specimen may be used for numerous situations of loading, may they be uniaxial or multiaxial, monotonic or cyclic, possibly for situations that cannot be realized in the laboratory for reasons of principle or for practical reasons. Slight modifications of the size distribution of the virtual aggregates and even the generation of different virtual specimens consisting of an identical ensemble of aggregates (so-called clones) are possible and

allow to repeat the numerical experiments under slightly different initial conditions any number of times.

This article concentrates on a detailed description of the generation of virtual specimens. An ad hoc approach to paste the particle ensembles is used in order to perform some tests for plausibility. We start with a first 1D approach to wave propagation and spall fracture, which leads in a quite natural way to the Distinct/Discrete Element Method.

2 A 1D DISCRETE ELEMENT APPROACH

Spallation experiments are performed in order to investigate the material behavior in situations of high compressive loading or impact. For that purpose the specimen is hit at one end by a Hopkinson pressure bar or similar device. Then a wave propagates through the specimen which under certain circumstances causes the specimen to split into fragments. Fig. 1 shows a specimen of cylindrical shape that was exposed to high compressive loading and fragmented into three pieces.

Figure 1: Concrete specimen, destroyed by spall fraction. (Photography: Ulrich van Stipriaan)

As a first approach to simulate the spallation phenomenon, the specimen is considered to be consisting of a number of pairwise mutually overlapping segments (or slices or *discrete elements*). All segments are supposed to have the same longitudinal extension or segment length a, and – at the beginning, i. e. at equilibrium – any two segments have the same overlapping area $\lambda_0\, a$, where the initial relative depth of penetration λ_0 is a small positive number (see Fig. 2). Then the initial length L_0 of the entire specimen (neither loaded in compression nor in tension) can be calculated by

$$L_0 = [N - \lambda_0(N-1)]\, a\ , \tag{1}$$

or, since it is more convenient to give the specimen a certain initial length, the segment length a can be calculated by

$$a = \frac{L_0}{N - \lambda_0(N-1)}\ . \tag{2}$$

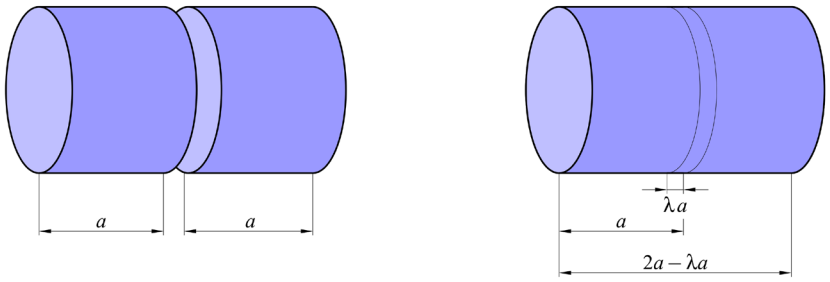

Figure 2: Geometrical relations for two non-overlapping and two overlapping segments.

The value of a depends on our choices for N and λ_0. λ_0 itself depends on N and different material parameters, which can be seen after it was explained what mechanical properties the virtual specimen is supposed to have.

The specimen will have a certain density ϱ, which allows to calculate its mass by

$$m = \varrho \, L_0 A \; , \tag{3}$$

where A denotes the cross-sectional area of the rod. If the total mass is equally distributed to the respective segments, the segment mass m_S is obtained by:

$$m_S = \varrho \, \frac{L_0 A}{N} \; . \tag{4}$$

When (slowly) loaded in tension, the specimen should behave as if consisting of a perfectly linear-elastic, not at all ductile material with modulus of elasticity E and maximum tensile strength σ_{max}. That means, there is a maximum tensile force F_{max} the specimen can withstand. When this force is exceeded it breaks into its N different segments at the same time. At this moment, the specimen has a length

$$L_{max} = N \, a \; , \tag{5}$$

which means that all regions of contact are stretched to the maximum, and all relative depths of penetration become zero. Thus, for the maximum tensile strain ϵ_{max} we obtain:

$$\epsilon_{max} = \frac{L_{max} - L_0}{L_0} = \frac{\lambda_0 (N-1) a}{[N - \lambda_0 (N-1)] \, a} \; . \tag{6}$$

For σ_{max}, E, and ϵ_{max} holds the following the simple relation, according to Hooke's law,

$$\sigma_{max} = E \, \epsilon_{max} \; , \tag{7}$$

from which the following formula for λ_0 can be obtained:

$$\lambda_0 = \frac{N}{N-1} \, \frac{1}{1 + \dfrac{E}{\sigma_{max}}} \, . \tag{8}$$

The specimen, spatially discretized in longitudinal direction, can be understood as a chain of mass points, pairwise connected by springs (and dampers, since real wave propagation dissipates energy). It can be shown, that for the inner segments (i. e. for all $N-2$ segments other than the leftmost and the rightmost segment) the following equations of motion are given by Newton's second law:

$$m_i \, \ddot{x}_i = \frac{x_{i-1} - 2x_i + x_{i+1}}{\lambda_0 a} \, F_{max} + \delta v_{i-1} - 2\delta v_i + \delta v_{i+1} \, , \tag{9}$$

where x_i and v_i denote the i-th segment's position and velocity, respectively, and δ is a universal dissipation coefficient (responsible for viscous damping). The formulae for the leftmost and the rightmost segment slightly differ from the formula above, you shouldn't care about this at this point.

Applying the well-known Stoermer-Verlet method for time integration, the problem can be posed in matrix notation as follows:

$$\mathbf{x}^{n+1} = \mathbf{x}^n + \Delta t \, \mathbf{v}^n - \frac{\Delta t^2}{2} \, \mathbf{M}^{-1} \left(\mathbf{Q} \, \mathbf{x}^n + \mathbf{q} + \mathbf{K^T D K} \, \mathbf{v}^n \right) , \tag{10}$$

$$\mathbf{v}^{n+1} = \left(\mathbf{I} + \frac{\Delta t}{2} \, \mathbf{M}^{-1} \mathbf{K^T D K} \right)^{-1} \left(\mathbf{v}^n - \frac{\Delta t}{2} \, \mathbf{M}^{-1} \left[\mathbf{Q} \, (\mathbf{x}^n + \mathbf{x}^{n+1}) + 2\mathbf{q} + \mathbf{K^T D K} \, \mathbf{v}^n \right] \right) . \tag{11}$$

Here $\mathbf{x}^n$ and $\mathbf{v}^n$ denote the vectors of segment positions and velocities at the n-th time step, Δt the step size for time integration, $\mathbf{M}$ and $\mathbf{D}$ are diagonal matrices containing segment masses and dissipation coefficients, respectively, $\mathbf{I}$ stands for the $N \times N$ identity matrix, and

$$\mathbf{Q} = \frac{F_{max}}{\lambda_0 a} \begin{pmatrix} 1 & -1 & & & \\ -1 & 2 & -1 & & \\ & \ddots & \ddots & \ddots & \\ & & -1 & 2 & -1 \\ & & & -1 & 1 \end{pmatrix} , \qquad \mathbf{q} = \frac{1-\lambda_0}{\lambda_0} F_{max} \begin{pmatrix} 1 \\ 0 \\ \vdots \\ 0 \\ -1 \end{pmatrix} . \tag{12}$$

The matrix $\mathbf{K}$, finally, is an $(N-1) \times N$ matrix responsible for dissipative interaction,

$$\mathbf{K} = \begin{pmatrix} 1 & -1 & & & \\ & 1 & -1 & & \\ & & \ddots & \ddots & \\ & & & 1 & -1 \end{pmatrix} . \tag{13}$$

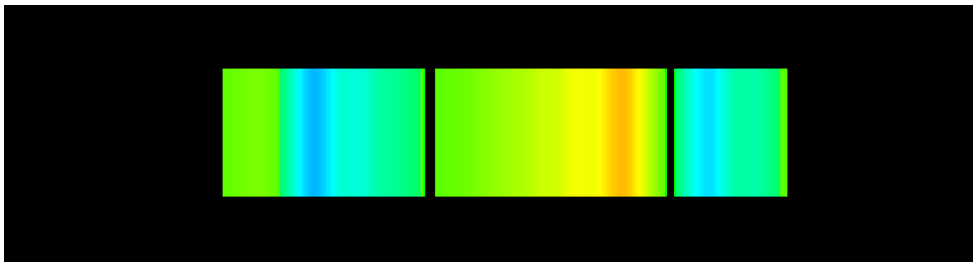

Figure 3: Virtual specimen after about 7 ms of simulation time.

Table 1: Parameters used in the 1D simulation of spall fracture

Parameter	Symbol	Value	Unit
Length	L_0	200	mm
Diameter	d	50	mm
Density	ϱ	0.0024	g/mm^3
Modulus of elasticity	E	37000	N/mm^2
Maximum tensile stress	σ_{max}	4.1	N/mm^2
Dissipation coefficient	δ	10	g/ms
Number of elements	N	200	–
Time step size	Δt	0.00025	ms

The model described can be implemented, for instance, in the MATLAB scripting language. Fig. 3 shows the simulation result for the model parameters given in Tab. 1. Within the first 0.355 ms the leftmost segment (or element or particle) was continuously accelerated to a velocity of 3 mm/ms which is equivalent to a momentum difference of 0.87 g mm/ms. The figure shows the virtual specimen after about 7 ms have been elapsed. The specimen spalled into three fragments. Colors indicate compressive (blue) and tensile (orange/yellow) strain at the respective positions of the specimen.

This 1D approach, of course, is much too simple to yield realistic simulation results. For instance no lateral strain is included in the model. Moreover, the fracture surfaces are not at all plane, but show a complicated, fractal structure. One would expect to obtain better simulation results by means of a 3D approach which takes into consideration concrete's heterogeneous nature. Fig. 4 shows the prototype of a cylindrical virtual specimen for usage in simulations of wave propagation and spall fracture, which raises the question how such specimen can be generated.

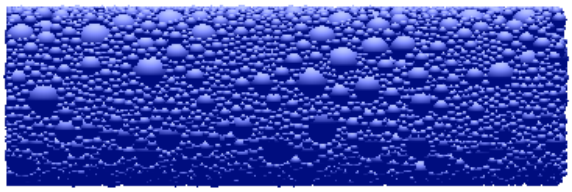

Figure 4: Virtual specimen for numerical simulations of spall fracture.

3 PARTICLE GENERATION AND INTERACTION

3.1 Particle Generation

Concrete aggregates are modelled as spherical particles of different diameter. The size distribution should approximate realistic sieving distributions for concrete. In this context several problems occur. First, realistic sieving distributions are obtained using a finite number of sieves (actually only a few), which makes the sieving result depending on the size distribution of the aggregates sieved. On the other hand, the well-known interpolations such as the Fuller parabola do not allow to construct suitable random generators.

3.2 Particle Interaction

The approach used for particle interaction is based on contact models for 2D polygon/polygon interaction as given by [1], [2], [3] and [4], for respective simulation results see also [5], [6] and [7]. In these models the magnitude of the repulsive contact force depends on the intersection area of two overlapping particles. This allows a permanent intersection at equilibrium if external forces are applied to the contact partners (Soft Contact approach). In case of 3D simulations the overlap area has to be replaced by the contact volume of the intersection of two spherical particles. Fig. 5 shows how the relative contact volume V_{rel}^{C} (i.e. the contact volume relative to the volume of the smaller particle) depends on the relative depth of penetration (i.e. the depth of penetration relative to the diameter of the smaller particle). The solid curve describes the special case of a particle contacting another particle of twice its diameter. The dashed lines show the extremal cases of two interacting particles of same diameter and a particle interacting with a "infinitely" larger particle (which represents the contact of a particle with a plane, a wall or a loading plate).

Besides the contact volume, the interaction of two particles with position and velocity vectors $\mathbf{x}_i$, $\mathbf{v}_i$ and $\mathbf{x}_k$, $\mathbf{v}_k$, respectively, depends on the distance vector

$$\mathbf{n} = \frac{\mathbf{x}_i - \mathbf{x}_k}{\|\mathbf{x}_i - \mathbf{x}_k\|} \tag{14}$$

and the relative velocity

$$\mathbf{v_{rel}} = \mathbf{v}_i - \mathbf{v}_k \,. \tag{15}$$

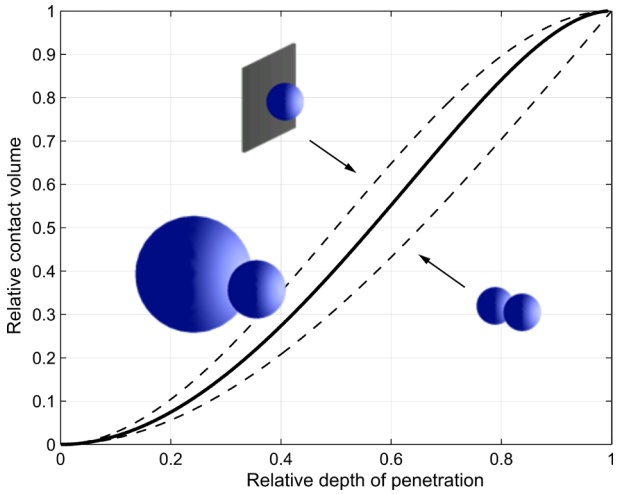

Figure 5: Relative contact volume in dependence of the relative depth of penetration.

The contact force resulting from particle interaction is composed by a normal and a tangential part:

$$\mathbf{F}^C = \mathbf{F}^C_\perp + \mathbf{F}^C_\parallel \,. \tag{16}$$

Using the projection $\mathbf{v}_\parallel$ of $\mathbf{v_{rel}}$ into the contact plane, which is described by the normal vector $\mathbf{n}$,

$$\mathbf{v}_\parallel = \mathbf{v_{rel}} - (\mathbf{v_{rel}} \cdot \mathbf{n})\,\mathbf{n}\,, \tag{17}$$

the components of $\mathbf{F}^C$ can be expressed by:

$$\mathbf{F}^C_\perp = f^C_\perp(V^C, \mathbf{v_{rel}})\,\mathbf{n}\,, \tag{18}$$

$$\mathbf{F}^C_\parallel = f^C_\parallel(\mathbf{v_{rel}})\,\frac{\mathbf{v}_\parallel}{\|\mathbf{v}_\parallel\|}\,. \tag{19}$$

Adding the terms for viscous damping yields:

$$f^C_\perp(V^C, \mathbf{v_{rel}}) = \frac{k}{d}\,(V^C_{rel} - \kappa)\,V_{min} - \gamma_\perp\, m_{eff}\, v_\perp\,, \tag{20}$$

$$f^C_\parallel(\mathbf{v_{rel}}) = -\gamma_\parallel\, m_{eff}\, v_\parallel\,. \tag{21}$$

In the formulae above denote:

- V_{min} the volume of the smaller particle,
- V^C_{rel} the relative contact volume, i.e. the ratio of the contact volume and the volume of the smaller particle,
- κ a parameter to manipulate the contact law (see below),

- k a parameter that allows to scale the contact force,
- d the characteristic length, $1/d = 1/d_i + 1/d_k$, where d_i, d_k are the respective diameters of the particles,
- m_{eff} the effective mass, $1/m_{eff} = 1/m_i + 1/m_k$, where m_i, m_k are the respective particle masses,
- $v_\perp$ and $v_\parallel$ the normal and tangential components of the particles' relative velocity,
- $\gamma_\perp$ and $\gamma_\parallel$ parameters that allow to control normal and tangential dissipative interaction.

There exist different approaches for modelling static friction (see, for instance, [1], [4] and [8]). Numerical investigations on the respective effects on the simulation results are on the way.

For each particle, the equation of motion is now schematically given by:

$$m_i \, \ddot{\mathbf{x}}_i = \sum_{k \neq i} \left(\mathbf{F}^C(\mathbf{x}_i, \mathbf{x}_k) - \gamma \, m_{eff} \, (\mathbf{v}_i - \mathbf{v}_k) \right) . \tag{22}$$

Thus the method requires the solution of an initial value problem for a system of ordinary differential equations of second order, which can be obtained by any suitable numerical integration scheme.

4 IMPLEMENTATION

The simulation code, written in C, is based on the code fragments given by [9]. A good part of the code is dedicated to runtime efficiency. The well-known Linked Cells strategy with some refinements described in [10] is used to reduce the computational effort. However, the great differences in particle size require some modifications since the cell width is dictated by the largest particle diameter. The simulation therefore uses two different meshes of linked cells, a coarser mesh for the larger particles and a finer one for the smaller particles, an idea that can be refined to a Hierarchical Linked Cells mechanism.

5 VIRTUAL SPECIMENS

5.1 Packing of virtual aggregates

The generation of virtual concrete specimens starts with the successive generation of layers of virtual aggregates above a virtual shuttering unit. Under the influence of gravitation and repulsive as well as dissipative interaction forces (particle/particle and particle/wall) densely packed particle ensembles of different size and geometry can be obtained. Fig. 6 shows three specimens with the same cross-sectional area, consisting of exactly the same ensemble of particles.

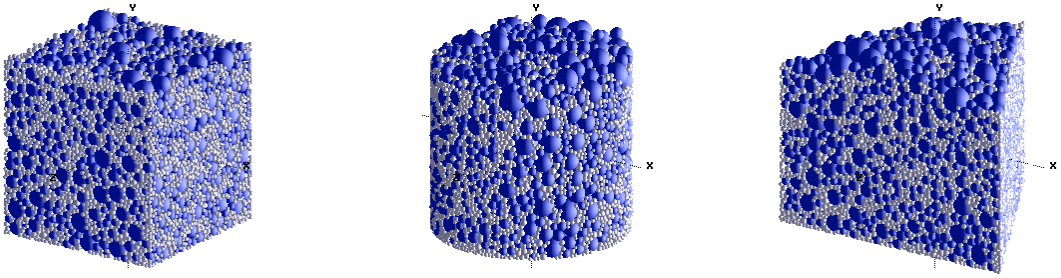

Figure 6: Cubic, cylindrical and prismatic specimens with the same cross-sectional area, generated by use of identical virtual aggregates. The simulation result is in good accordance with Cavalieri's principle.

5.2 Generation of virtual specimens

In order to obtain virtual specimens that keep shape when the respective shuttering unit is removed, cohesive interaction between adjacent particles has to be added to the model. One possibility to achieve this goal is to add a network of immaterial bars to the model (see, for instance, [4]).

Here the following ad hoc approach is chosen, which makes the repulsive and the cohesive interaction forces depending only on the amount of particle intersection: A certain, small value is subtracted from the relative contact volume, which formally allows negative values for the contact volume. This has to be done sufficiently slow in order to avoid premature crack evolution inside of the virtual specimens (see Fig. 7).

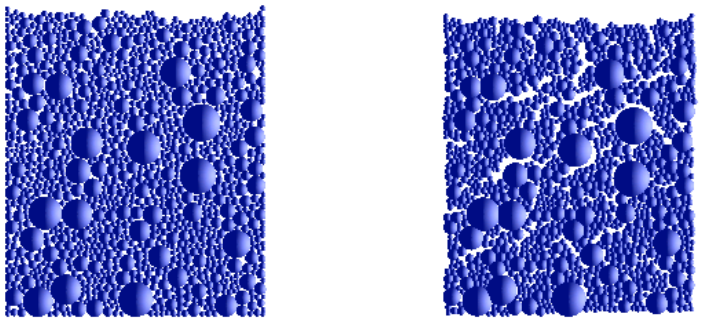

Figure 7: A 2D virtual specimen shortly before and immediately after cohesive interaction has been activated in an abrupt manner.

The virtual specimens obtained by this procedure keep shape and act together like a rigid body when being let loose or been thrown (Fig. 8).

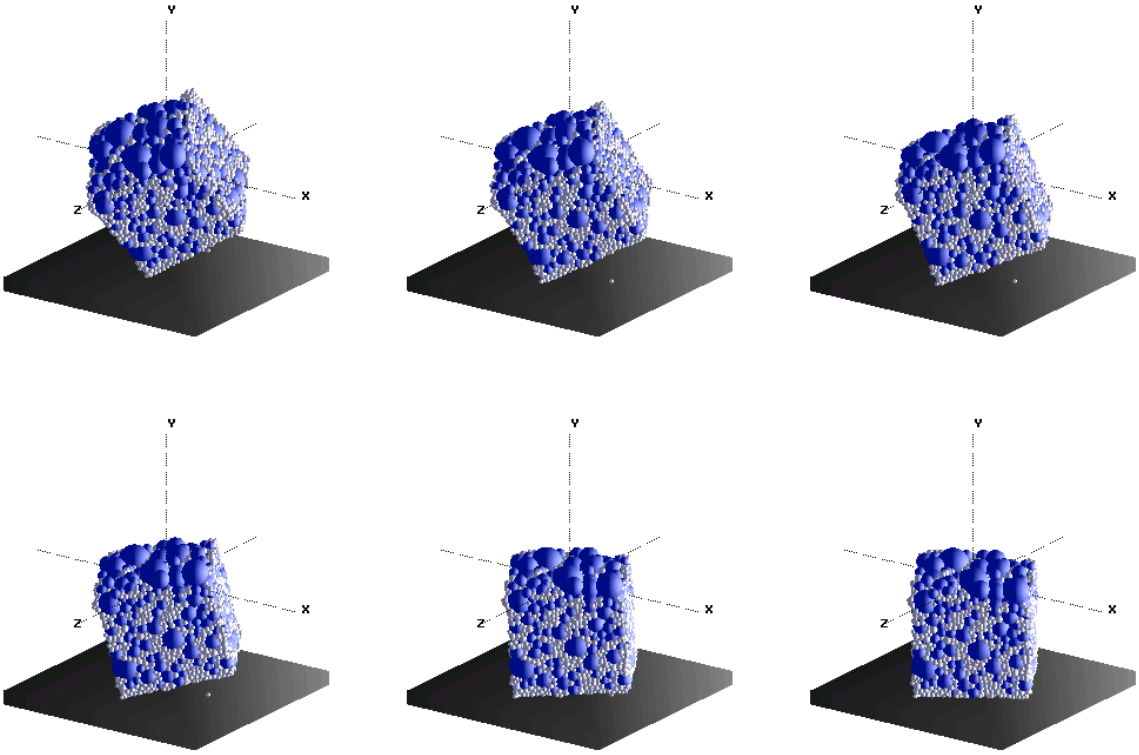

Figure 8: Even without static friction included, this specimen keeps shape when being dropped and hitting a loading plate.

Up to a certain amount of loading, the virtual specimens show elastic material behavior when loaded in compression or tension, while crack evolution and propagation can be observed when the applied forces are furthermore increased (Fig. 9).

6 CONCLUSIONS

The model described allows to generate densely packed ensembles of spherical particles with size distributions that approximate realistic sieving distributions for concrete aggregates. The approach can neither compete with sophisticated models of granular flow, nor with models that are tailored to special cases of loading. On the other hand, it contains no artificial supplements such as bars or other, and allows to detect crack evolution directly. Further efforts have to be made in order to obtain better simulation results, in particular the addition of a suitable model of static friction.

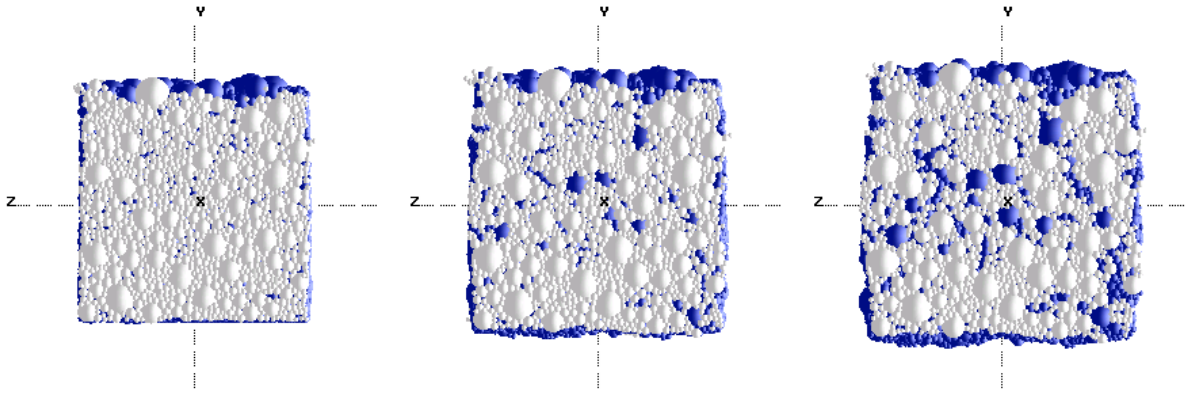

Figure 9: Crack evolution of a virtual specimen loaded in compression. Particles in the area of load application are drawn white in order to visualize the crack pattern.

7 ACKNOWLEDGEMENTS

This work was supported by the Deutsche Forschungsgemeinschaft (DFG). We thank Evans Amponsah, Strahinja Djukanovic and Trung Luu for their support in performing parameter studies and for the visualization of some of the simulation results. Fig. 1 shows a real-world specimen destroyed by spallation, obtained by experimental setup of Tino Kühn, Institute of Concrete Structures.

REFERENCES

[1] Kohring, G.A., Melin, S., Puhl, H., Tillemans, H.J. and Vermöhlen, W.: Computer simulations of critical, non-stationary granular flow through a hopper. *Computer Methods in Applied Mechanics and Engineering* (1995) **124**:273–281.

[2] Feng, Y.T. and Owen, D.R.J.: A 2D polygon/polygon contact model: Algorithmic aspects. *Engineering Computations* (2015) **21**:265–277.

[3] D'Addetta, G.A., Kun, F. and Ramm, E.: On the application of a discrete model to the fracture process of cohesive granular materials. *Granular Matter* (2002) **4**:77–90.

[4] D'Addetta, G.A.: *Discrete Models for Cohesive Frictional Materials*. Ph.D. Thesis, Universität Stuttgart (2004).

[5] Beckmann, B., Schicktanz, K., Reischl, D., and Curbach, M.: DEM simulation of concrete fracture and crack evolution. *Structural Concrete* (2012) **13**:213–220.

[6] Beckmann, B., Schicktanz, K. and Curbach, M.: DEM Simulation of Concrete Fracture Phenomena. *ICMM3 – 3rd International Conference on Material Modelling*. Warsaw, Poland (2013) no. 36.

[7] Beckmann, B., Schicktanz, K. and Curbach, M.: Discrete Element Simulation of Concrete Fracture and Crack Evolution. *SSCS 2012 – International Conference on Numerical Modelling Strategies for Sustainable Concrete Structures*. Aix-en-Provence, France (2012) no. 301.

[8] Tran, V.T., Donzé, F.-V. and Marin, P.: A discrete element model of concrete under high triaxial loading. *Cement & Concrete Composites* (2011) **33**:936–948.

[9] Griebel, M., Knapek, S., Zumbusch, G. and Caglar, A.: *Numerische Simulation in der Molekül̈dynamik*. Springer (2004).

[10] Munjiza, A.A.: *The Combined Finite-Discrete Element Method*. Wiley (2004).